How to cite: *Angew. Chem. Int. Ed.* **2023**, *62*, e202314280
doi.org/10.1002/anie.202314280

Glycomimetics

Tetra- and Hexavalent Siglec-8 Ligands Modulate Immune Cell Activation

Gabriele Conti, Anne Bärenwaldt, Said Rabbani, Tobias Mühlethaler, Mirza Sarcevic, Xiaohua Jiang, Oliver Schwardt, Daniel Ricklin, Roland J. Pieters, Heinz Läubli,* and Beat Ernst**

Abstract: Carbohydrate-binding proteins are generally characterized by poor affinities for their natural glycan ligands, predominantly due to the shallow and solvent-exposed binding sites. To overcome this drawback, nature has exploited multivalency to strengthen the binding by establishing multiple interactions simultaneously. The development of oligovalent structures frequently proved to be successful, not only for proteins with multiple binding sites, but also for proteins that possess a single recognition domain. Herein we present the syntheses of a number of oligovalent ligands for Siglec-8, a monomeric I-type lectin found on eosinophils and mast cells, alongside the thermodynamic characterization of their binding. While the enthalpic contribution of each binding epitope was within a narrow range to that of the monomeric ligand, the entropy penalty increased steadily with growing valency. Additionally, we observed a successful agonistic binding of the tetra- and hexavalent and, to an even larger extent, multivalent ligands to Siglec-8 on immune cells and modulation of immune cell activation. Thus, triggering a biological effect is not restricted to multivalent ligands but could be induced by low oligovalent ligands as well, whereas a monovalent ligand, despite binding with similar affinity, showed an antagonistic effect.

Introduction

Siglecs (sialic acid-binding immunoglobulin-like lectins) are a family of lectins that participate in the discrimination between 'self' and 'non-self' and regulate the function of cells in the innate and adaptive immune system by recognizing glycan ligands.[1] They exhibit a sialic acid binding N-terminal domain, one or more C2-set immunoglobulin domains, and a cytoplasmic tail.[2] The cytoplasmic tail of most Siglecs contains an immunoreceptor tyrosine-based inhibitory motif (ITIM), which functions as an inhibitory receptor and suppresses activation signals. Ligand binding induces phosphorylation of the tyrosine motif by an Src family kinase, resulting in the recruitment of SH2 (SRC homology 2) domain containing phosphatases.[3] These inhibit cellular processes through inactivation of essential kinases and, therefore, can modulate crucial immune responses.[4] In their resting state, most Siglecs are engaged in *cis* interactions with sialylated glycans expressed on the surface of the same cell.[5] As a result, Siglecs are essentially masked and can only interact with *trans* ligands that display sufficient affinity or avidity to outcompete the *cis* interactions.[6]

Although different inhibitory Siglecs have different biochemical mechanisms,[1b] a generalized model that sialoglycan-induced Siglec clustering leads to inhibition is the basis for many investigations in this area.[7] Siglec-8, expressed on eosinophils, mast cells, and weakly on basophils, has proven to be a promising target for the treatment of a variety of eosinophil- and mast-cell-associated disorders, such as asthma, chronic rhinosinusitis, chronic urticaria, hypereosinophilic syndromes, mast cell and eosinophil malignancies, and eosinophilic gastrointestinal disorders.[8] The engagement of Siglec-8 with a monoclonal antibody[9] or polyvalent sialic acid mimetics[10] induces apoptosis/cell death of eosinophils and inhibits mast cell degranulation. These findings could be confirmed when anti-Siglec-8 antibodies were administrated in vivo to humanized and trans-

[*] Dr. G. Conti, Dr. S. Rabbani, Dr. X. Jiang, Dr. O. Schwardt, Prof. Dr. D. Ricklin, Prof. Dr. B. Ernst
Molecular Pharmacy Group, Department of Pharmaceutical Sciences, University of Basel
Klingelbergstrasse 50, 4056 Basel (Switzerland)
E-mail: beat.ernst@unibas.ch
Dr. G. Conti, Prof. Dr. R. J. Pieters
Chemical Biology and Drug Discovery Group, Department of Pharmaceutical Sciences, Utrecht University
Universiteitsweg 99, 3584 CG Utrecht (The Netherlands)
E-mail: r.j.pieters@uu.nl
Dr. A. Bärenwaldt, M. Sarcevic, Prof. Dr. H. Läubli
Laboratory for Cancer Immunotherapy, Department of Biomedicine, University of Basel
Hebelstrasse 20, 4051 Basel (Switzerland)
and
Division of Medical Oncology, University Hospital Basel
Petersgraben 4, 4051 Basel (Switzerland)
E-mail: Heinz.laeubli@unibas.ch
Dr. T. Mühlethaler
Biophysics Facility, Department Biozentrum, University of Basel
Spitalstrasse 41, 4056 Basel (Switzerland)

genic mice selectively expressing Siglec-8 on eosinophils and mast cells. Currently, a humanized IgG1 antibody against Siglec-8 (AK002, lirentelimab), which acts as Siglec-8 agonist, depletes eosinophils through antibody-dependent cellular cytotoxicity[11] and inhibits mast cell activation, is in clinical development for mast-cell- and eosinophil-mediated diseases.[9,12]

A promising alternative to targeting Siglec-8 with antibodies involves the multivalent display of Siglec ligands on liposomes,[10a] polymers,[10b,c] or nanoparticles.[10d] Thus, it was shown that apoptosis can be initiated by treating eosinophils with a synthetic polyvalent Siglec-8 ligand,[11] and immunohistochemical analyses revealed an up-regulation of Siglec-8 ligands in inflamed compared to healthy tissue.[13] Additionally, Siglec-8 ligands could be presented on liposomes. When encapsulating drugs, such liposomes could be exploited for the delivery of their payloads to eosinophils, thanks to their endocytic activity.[14] Alternatively, liposomes simultaneously displaying Siglec-8 ligands and allergens could provide a useful strategy for building up tolerance and desensitize immune cells towards specific antigens, thereby preventing the risk of anaphylactic shocks.[10d]

Although all Siglecs interact with sialic acid containing glycoproteins and glycolipids, individual family members exert preferential binding to distinct sialic acid linkages and underlying glycan structures.[1a] Bochner et al. showed that Siglec-8 recognizes the tetrasaccharide 6′-sulfo-sialyl Lewis^x (**1**; Figure 1),[15] however, due to the flat and solvent-exposed binding site only with an affinity in the submillimolar range.[16] Similar to other natural Siglec ligands,[17] 6′-sulfo-sialyl Lewis^x (**1**) has been successfully developed into a series of glycomimetics that exhibit low micromolar affinity.[18]

Herein, we report the syntheses of a series of oligo- and polyvalent Siglec-8 ligands with scaffolds of different valencies and flexibilities. When characterizing their properties, special focus was set on determining the thermodynamic fingerprint of their interactions with Siglec-8 and assessing their biological function using an immune-cell-based assay.

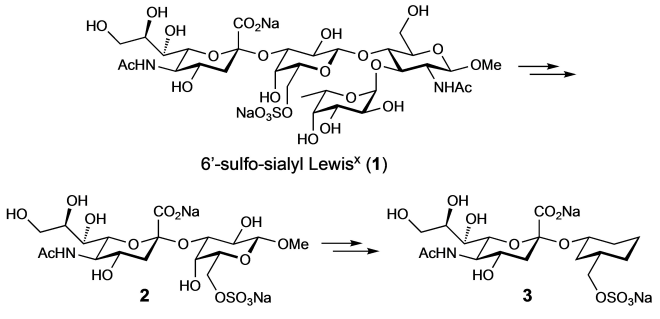

Figure 1. The natural epitope 6′-sulfo-sialyl Lewis^x (**1**), which binds to the carbohydrate recognition domain (CRD) of Siglec-8, and the derived glycomimetics **2** and **3**.[18b]

Results and Discussion

When the Fucα(1–3)Glc*N*Ac moiety was split from 6'-sulfo-sialyl Lewis^x (**1**, $K_D = 279\ \mu M$, Figure 1), the resulting disaccharide **2** ($K_D = 574\ \mu M$) suffered only from a two-fold reduction in affinity, indicating that the contribution to binding of the Fucα(1–3)Glc*N*Ac disaccharide is almost completely compensated by the reduction of desolvation enthalpy and conformational entropy.

In a second step, the galactose (Gal) moiety in **2** was replaced by (1*R*,3*S*)-3-(hydroxymethyl)cyclohexan-1-ol, that is, with a conformationally stabilized 1,4-butanediol linker to the sulfate, leading to mimetic **3**, which exhibits an almost two-fold improvement of affinity ($K_D = 259\ \mu M$). Apparently, neither the ring oxygen nor the aglycone or the hydroxyls in the 2- and 4-position essentially contribute to binding.[18b]

To further enhance binding, an oligo- and multivalent presentation of the carbohydrate ligand was explored. In this way, clustering of Siglec-8 in microdomains can be induced, which is required for triggering the biological response.[6] In addition, an oligo- and multivalent ligand with a proper spatial presentation of the individual epitopes increases its local concentration to enable fast rebinding upon dissociation.[19]

In order to achieve oligo- and multimeric presentations of epitope **3**, an additional exit vector is required to explore the chemical space. Importantly, the vector should not interfere with or preclude binding of the key functionality of the epitope. For this purpose, we extended the carbocycle with an additional hydroxy group that mimics the β1-4 glycosidic linkage between the Gal and *N*-acetyl-glucosamine (Glc*N*Ac) moieties present in the parent tetrasaccharide **1**.

Synthesis of the Carbocyclic Gal Mimetic

The synthesis of the glycosyl acceptor **14** equipped with a side chain for oligomerization started from commercial 3,5-dihydroxybenzoic acid (Scheme 1). After esterification (→ **5**), rhodium-catalyzed hydrogenation at 100 °C and with 90 atm H_2 for 72 h quantitatively yielded the all-*cis* derivative **6**. Subsequent enzymatic asymmetrization[20] with porcine pancreatic lipase type II (PPL-II) and vinyl acetate led to the enantiomer **7** with an overall chemical yield of 95 % over three steps. Its optical rotation was in agreement with the reported value.[21] In addition, to determine the enantiomeric purity, the corresponding Mosher ester **8** was formed, while the non-asymmetric monoacetylation of **6** subsequently esterified with Mosher chloride provided the diastereoisomeric mixture as reference. Surprisingly, ^{19}F NMR analysis was inconclusive, as only a single peak could be detected for the Mosher derivative of racemic **6**, not allowing to distinguish the two diastereomers. However, in the ^1H NMR spectrum, the peaks of the signals for the methyl ester and acetate were split for the two diastereoisomers, indicating an enantiomeric excess >99 % for **7** (for details, see the Supporting Information). Subsequent

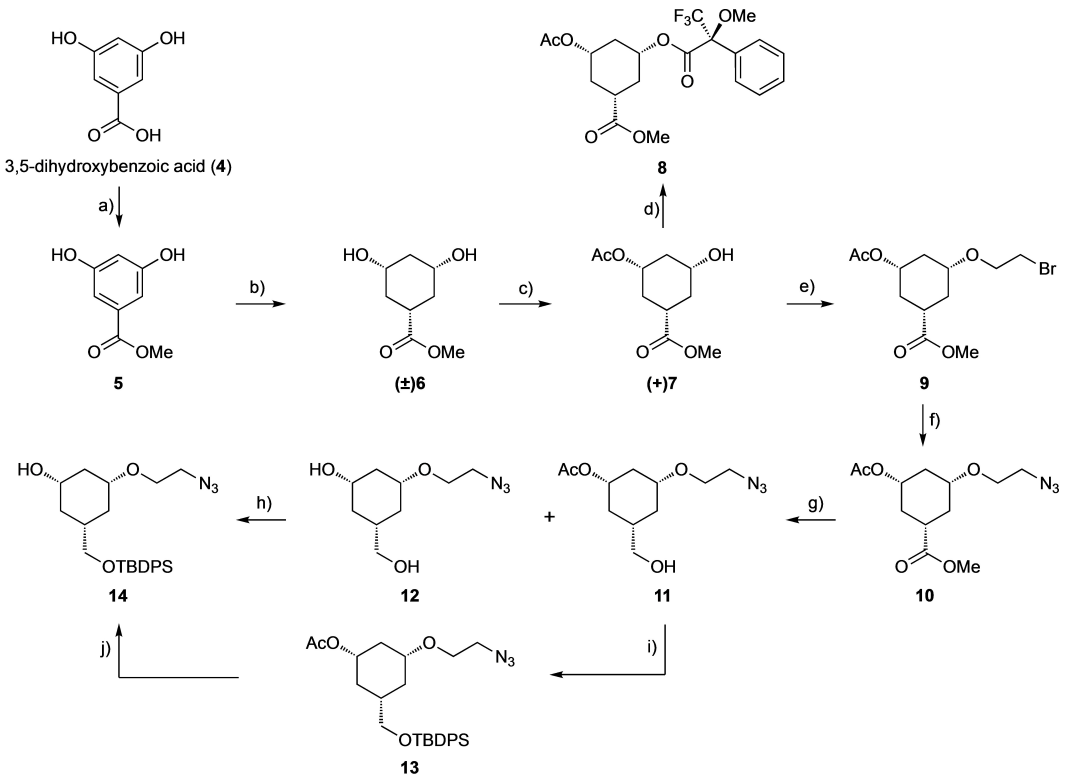

Scheme 1. Synthesis of the glycosyl acceptor **14**. Reagents and conditions: a) H_2SO_4, MeOH, reflux, 4 days (quant.); b) Rh/Al_2O_3, H_2 (90 bar), MeOH, 100 °C, 72 h (quant.); c) vinyl acetate, PPL (lipase from porcine pancreas, type II), room temperature, 20 h (95 %); d) (*R*)-(−)-MTPA-Cl, CH_2Cl_2, 0 °C→rt; e) 2-bromoethyltriflate, DIPEA (*N*,*N*-diisopropylethylamine), toluene, 25→100 °C, 48 h (quant.); f) NaN_3, DMF (dimethylformamide), room temperature, 24 h (quant.); g) $LiBH_4$, THF/MeOH, 0 °C→rt, 18 h (**11**, 19 % and **12**, 45 %) h) TBDPSCl (*tert*-butyldiphenylsilylchloride), DMAP (4-dimethylaminopyridine), imidazole, room temperature, 43 h (71 %); i) TBDPSCl, DMAP, imidazole, room temperature, 19 h; j) NaOH (aq), MeCN (acetonitrile), room temperature, 19 h (71 % from **11**). For experimental details, see the Supporting Information.

functionalization of the free hydroxyl group with freshly prepared 2-bromoethyltriflate[22] afforded **9**, and by nucleophilic substitution with sodium azide compound **10**. Treatment of **10** with a stoichiometric amount of lithium borohydride resulted in a mixture of both alcohol **11** and diol **12** in 19 % and 45 % yield, respectively. To avoid double silylation, the *tert*-butyldiphenylsilyl (TBDPS) protection of the primary alcohol in diol **12** (→**14**) had to be performed at 0 °C and lasted 43 h. Because the acetate in **11** acted as protecting group, silylation could be performed at rt, leading to **13** in only 19 h. The final deacetylation with aq. sodium hydroxide yielded **14**.

The aim of this work was to compare the monovalent ligand **3** with its oligo- and multivalent presentations and to study the impact of shape and flexibility of the scaffolds used. Therefore, the Gal mimetic **14** was sialidated using donor **15**[23] (Scheme 2) to give pseudodisaccharide **16** in 50 % yield. Subsequent treatment with HF to remove the TBDPS protection (→**17**) and sulfation of the primary hydroxyl group gave **18** in almost quantitative yield. Final deprotection with aqueous NaOH provided the monovalent ligand **19**.

For facilitating the simultaneous formation of multiple interactions, the central scaffold used for the oligo- and multivalent presentation of the carbohydrate epitope has to meet specific criteria regarding rigidity versus flexibility to allow the proper spatial arrangement of the epitopes while keeping the entropic penalty as low as possible. Therefore, a number of flexible, branched, carbocylic and aromatic scaffolds were decorated with the carbohydrate epitope **19** by click chemistry (Scheme 3).

The alkyne-equipped scaffolds **S11**–**S20** to be used for CuAAC (copper-catalyzed azide-alkyne cycloaddition) coupling[24] with **19** were obtained by treatment of the corresponding alcohols **S1**–**S10** with propargyl bromide under basic conditions (Scheme 3). Various bases from mild K_2CO_3 for the phenolic hydroxyl groups to NaH or KOH for the primary alcohols were applied (see the Supporting Information for experimental details). Click CuAAC reactions yielding the oligovalent compounds **20**–**30** were performed using copper(I) bromide as Cu^I source and tris((1-benzyl-4-triazolyl)methyl)amine (TBTA) as stabilizing agent to prevent copper oxidation and disproportion.[25]

For the synthesis of the multivalent representative **33**, compound **19** was further modified to enable the attachment to a L-lysine polymer (PLL), employing a previously published procedure that used γ-thiobutyrolactone as linker for attaching amines to chloroacetyl derivatives of PLL (Scheme 4).[26] First, hydrogenation of **19** led to the primary amine **31**, which was then treated with γ-thiobutyrolactone

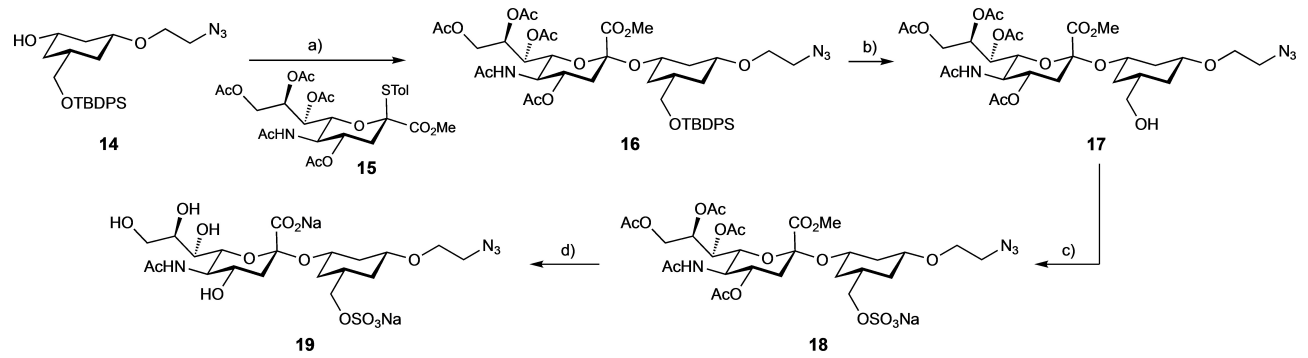

Scheme 2. Synthesis of monovalent epitope **19**. Reagents and conditions: a) NIS (*N*-iodosuccinimide), TfOH (triflic acid), MS 3 Å, MeCN, −40 °C, 14 h (50%); b) HF·pyr, pyridine, 0 °C, 7 h (95%); c) SO_3·pyridine, DMF (dimethylformamide), room temperature, 5.5 h (99%); d) NaOH (aq), room temperature, 48 h (84%). For experimental details, see the Supporting Information.

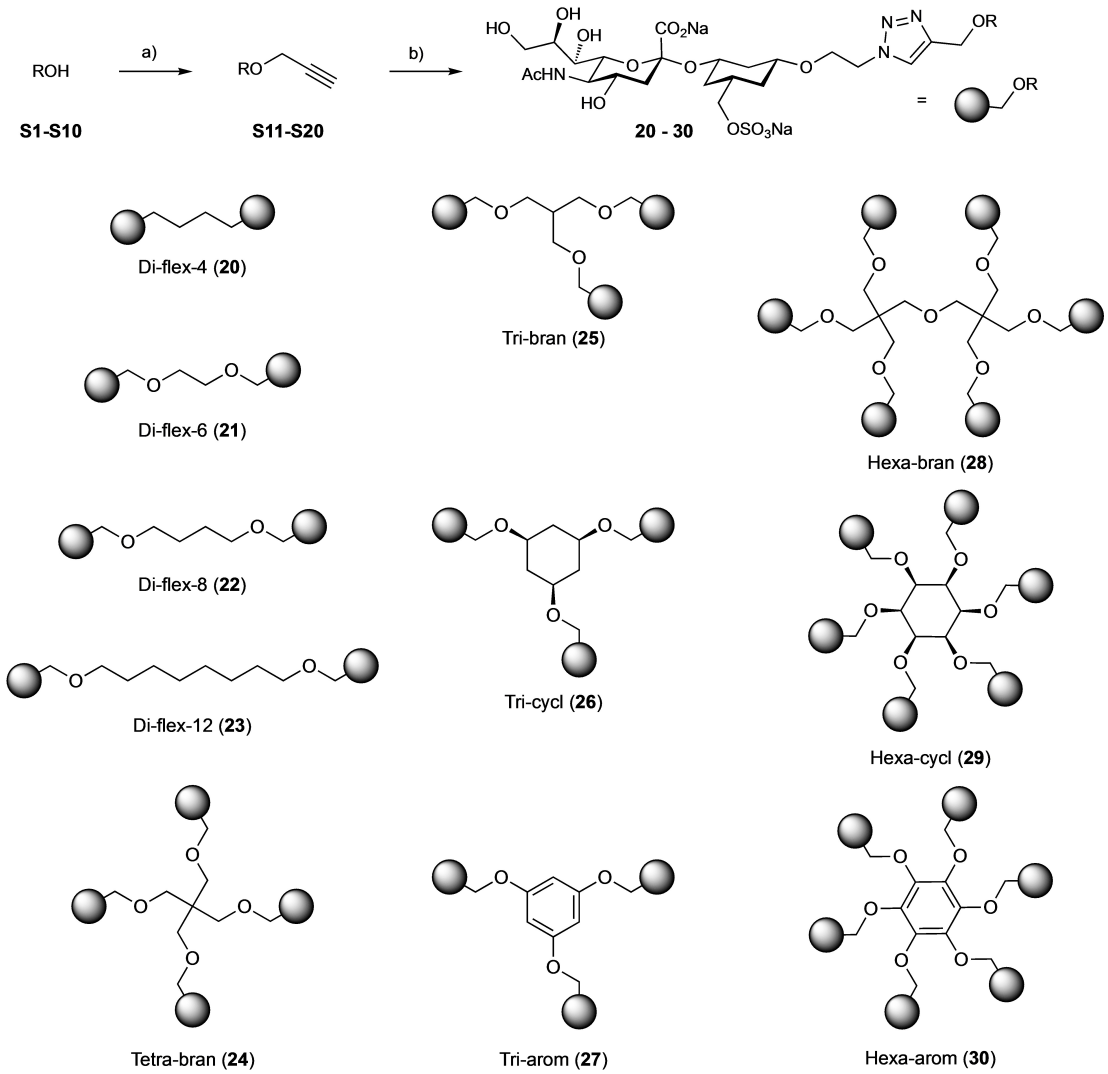

Scheme 3. General synthesis of oligomeric ligands with distinct scaffolds. Reagents and conditions: a) propargyl bromide, base, DMF, 0 °C→rt (5–90%); b) **19**, copper(I) bromide, TBTA, MeCN/H_2O, room temperature, overnight (19–63%). The acronyms indicate the valency of the ligand, the type of scaffold [flexible with number of atoms (flex-No), branched (bran), cyclohexane-based (cycl), or benzene-based (arom)]. Compound Di-flex-4 (**20**) was synthesized from commercially available 1,7-octadiyne. For experimental details, see the Supporting Information.

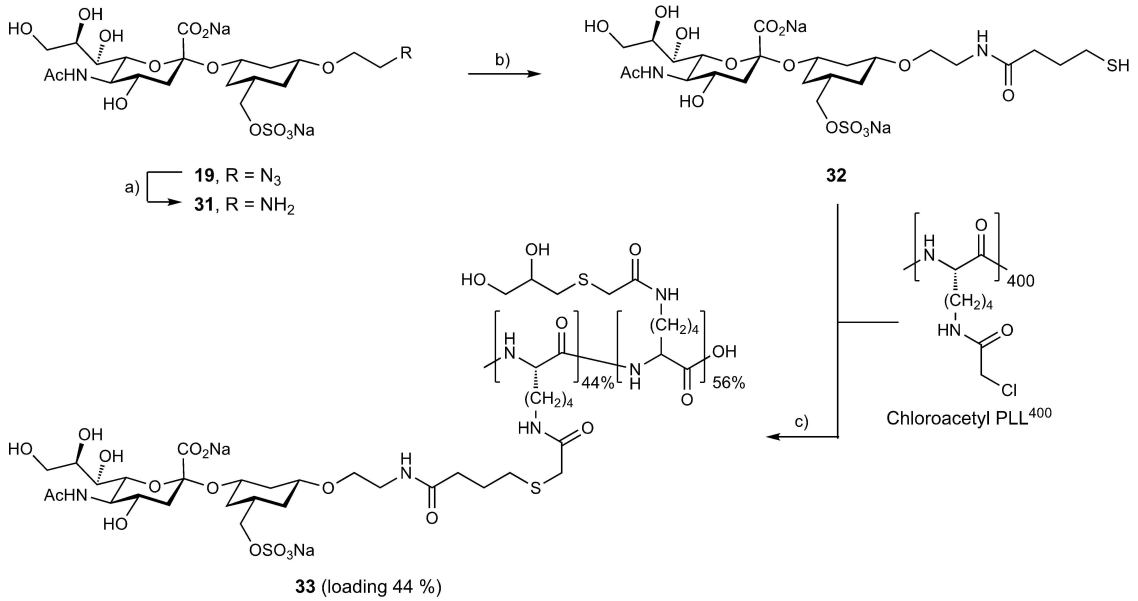

Scheme 4. Synthesis of glycopolymer **33**. Reagents and conditions: a) $Pd(OH)_2/C$, H_2 (1 atm), H_2O, rt, 24 h (96%); b) γ-thiobutyrolactone, NaOH, $MeOH/H_2O$, rt, 24 h (45%); c) DBU (1,8-diazabicyclo[5.4.0]undec-7-ene), DMF/H_2O, rt, 1 h; then thioglycerol, Et_3N (triethylamine), rt, overnight (91%, loading 44%). For experimental details, see the Supporting Information.

yielding the functionalized ligand **32**. Finally, chlorine substitution on chloroacetyl PLL^{400} provided polymer **33**, the loading of which was determined by ^1H NMR spectroscopy to be 44 % (see the Supporting Information for details).

Qualitative Binding Assessment to Siglec-8 CRD with NanoDSF

For the qualitative assessment of the binding of oligovalent ligands to the CRD of Siglec-8, nanoscale differential scanning fluorimetry (nanoDSF) was employed. Thus, the protein was incubated with a constant concentration of ligand, and the thermal denaturation profile was measured by monitoring changes of the fluorescence signal of the protein's aromatic residues as a function of temperature. Depending on the relative affinity, a ligand bound to the protein stabilizes its native state, causing a shift of the apparent melting temperature T_m to higher values.[27]

NanoDSF results for the various ligands are summarized in Table 1 (and Figure S3, Supporting Information). While the Siglec-8-CRD alone showed a T_m of 45.5 °C, incubation with the lead glycomimetic **3** or the monovalent ligand **19** resulted in ΔT_m shifts of +2.4 and +2.2 °C, respectively. The small difference of the ΔT_ms indicates that the additional azidoethyloxy substituent in **19** is not interfering with the protein and, thus, is ideally suited to link the carbohydrate epitope to the scaffolds. For the oligovalent compounds, positive temperature shifts with intensities increasing with rising valencies were obtained.

Since both protein and ligand are present in solution and can freely move, multivalent ligands may bind, in addition to statistical rebinding, to more than one protein, leading to aggregation phenomena. Since polymer **33** displays 176 epitopes, the actual concentration of epitopes, and therefore the T_m shift, is considered as comparable to the monovalent ligands **3** and **19**.

Table 1: T_m and ΔT_m (relative to reference compound **3**) values for various ligands. Siglec-8-CRD was used at a concentration of 20 μM and incubated with 1 mM of each ligand except **33**. For polymer **33**, the assay concentration was 5 μM and therefore 200-fold lower.

Compound	T_m [°C]	ΔT_m [°C]
Siglec-8-CRD	45.5	–
3 (reference compound)	47.9	+2.4
Monovalent **19**	47.7	+2.2
Di-flex-4 (**20**)	50.8	+5.3
Di-flex-6 (**21**)	52.3	+6.8
Di-flex-8 (**22**)	49.2	+3.7
Di-flex-12 (**23**)	49.7	+4.2
Tri-bran (**25**)	50.5	+5.0
Tri-cycl (**26**)	50.0	+4.5
Tri-arom (**27**)	50.8	+5.3
Tetra-bran (**24**)	51.2	+5.7
Hexa-bran (**28**)	55.8	+10.3
Hexa-cycl (**29**)	55.2	+9.7
Hexa-arom (**30**)	55.1	+9.6
Glycopolymer **33**	47.5	+2.0

Thermodynamic Characterization of Ligands

Besides the qualitative analysis of binding by nanoDSF, a more detailed and quantitative analysis was obtained by isothermal titration calorimetry (ITC), providing informa-

tion on binding affinity and thermodynamics at the same time. According to Table 2, the affinity trend in ITC measurements largely follows the increase in the number of interacting epitopes of the oligomers. Indeed, divalent compounds gained on average a 5.1-fold increase in affinity compared to the monovalent ligand, while these benefits are 14.2-, 16.1- and 25.9- fold for tri-, tetra- and hexavalent ligands, respectively.

The enthalpies ($\Delta H°$) per epitope of the oligovalent ligands are within a narrow range ($\Delta H°$/epitope = −27.8 ± 2.5 kJ·mol^{-1}), indicating comparable enthalpy contributions from each epitope when compared to the monovalent ligand **19**. The small deviations are likely related to desolvation enthalpies ($\Delta H°_{solv}$) stemming from the various scaffolds.

Furthermore, affinities also depend on the nature and flexibility of the scaffold. As expected, entropy costs increase with valency but are cancelled out by enthalpy contributions. Surprisingly, the entropy costs related to branched, cyclic and aromatic scaffolds do not show any tendency. In addition, within a valency group, affinities vary only marginally, that is, within a factor of 2.1 for divalent to 1.3 for hexavalent ligands, probably as a result of entropy/enthalpy compensation.[28]

However, much larger deviations (between 10.4 to 24.7 kJ·mol^{-1}) were registered for the entropy penalties per epitope. Whereas for the divalent ligands **20**–**23** the average entropy penalty per epitope is rather small (14.3 ± 3.0 kJ·mol^{-1}), it increases steadily with growing valency to

Table 2: Thermodynamic fingerprints, binding affinities, and stoichiometry of the interaction of oligovalent ligands with the Siglec-8-CRD.[a]

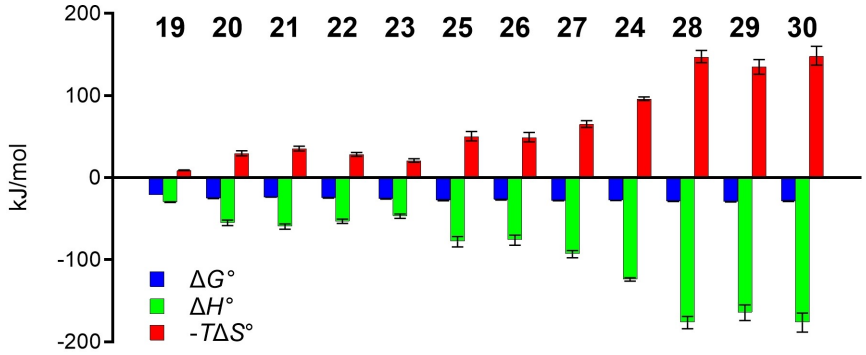

Compound	K_D [μM]	$\Delta G°$ [kJ·mol^{-1}]	$\Delta H°$ [kJ·mol^{-1}]	$\Delta H°$/epitope [kJ·mol^{-1}]	$-T\Delta S°$ [kJ·mol^{-1}]	$T\Delta S°$/epitope [kJ·mol^{-1}]	*N*-value (fixed)
19	230 (225–235)	−20.8 (−20.8–−20.7)	−29.7 (−30.1–−29.4)	−29.7	8.9 (8.6–9.3)	8.9	1
Di-flex-4 (**20**)	37.7 (33.2–42.7)	−25.2 (−25.6–−24.9)	−54.8 (−58.2–−51.6)	−27.4	29.5 (26.7–32.7)	14.8	0.5
Di-flex-6 (**21**)	64.6 (58.9–70.8)	−23.9 (−24.1–−23.7)	−59.3 (−62.6–−56.2)	−29.7	35.4 (32.5–38.5)	17.7	0.5
Di-flex-8 (**22**)	47.7 (43.4–54.5)	−24.7 (−24.9–−24.4)	−52.9 (−55.6–−50.4)	−26.5	28.3 (26.0–30.7)	14.2	0.5
Di-flex-12 (**23**)	29.8 (25.9–34.1)	−25.8 (−26.2–−25.5)	−46.7 (−49.4–−44.2)	−23.4	20.8 (18.7–23.2)	10.4	0.5
Tri-bran (**25**)	15.1 (12.3–18.5)	−27.5 (−28.0–−27.0)	−77.6 (−84.3–−71.8)	−25.9	50.1 (44.8–56.3)	16.7	0.333
Tri-cycl (**26**)	20.2 (16.9–24.1)	−26.8 (−27.2–−26.4)	−75.7 (−82.2–−70.1)	−25.2	48.9 (43.8–55.0)	16.3	0.333
Tri-arom (**27**)	13.2 (11.6–14.9)	−27.9 (−28.2–−27.6)	−93.0 (−97.6–−88.8)	−31.0	65.2 (61.3–69.4)	21.7	0.333
Tetra-bran (**24**)	14.3 (13.7–15.0)	−27.6 (−27.8–−27.5)	−124 (−126–−122)	−31.0	96.2 (94.1–98.4)	24.1	0.25
Hexa-bran (**28**)	9.19 (8.30–10.2)	−28.7 (−29.0–−28.5)	−176 (−184–−169)	−29.3	147 (140–155)	24.5	0.167
Hexa-cycl (**29**)	7.60 (6.60–8.75)	−29.2 (−29.6–−28.9)	−164 (−174–−155)	−27.3	135 (126–144)	22.5	0.167
Hexa-arom (**30**)	9.90 (8.59–11.5)	−28.6 (−28.9–−28.2)	−176 (−188–−165)	−29.3	148 (137–160)	24.7	0.167

[a] Error estimates resemble the 95% confidence interval from global fitting of two or more independent experiments (see the Supporting Information for details).

$24.5 \pm 1.2\ kJ \cdot mol^{-1}$ for the hexavalent ligands **28**–**30** and roughly follows the increase of the functional valency.

The entropy is composed of solvation, conformational and mixing entropy (eq. 1).

$$\Delta S^{\circ}_{obs} = \Delta S^{\circ}_{solv} + \Delta S_{conf} + \Delta S_{mix} \quad (1)$$

Since oligovalent structures are associated with increasing numbers of water molecules to be released into bulk solvent, increasingly favorable $-T\Delta S^{\circ}_{solv}$ values can be expected. The contributions to the conformational entropies $-T\Delta S_{conf}$ obviously depend on linker characteristics and are in general difficult to estimate. An exception are the divalent ligands. With the 12-atom linker in **23**, two binding sites can be reached without severely affecting the linker's flexibility, whereas shorter linkers as in the ligands **20**–**22** loose flexibility resulting in increased conformational entropy penalties. Finally, ΔS°_{mix} includes the loss of translational and rotational degrees of freedom. For N Siglec-8+ 1 N-valent ligand, ΔS°_{mix} is given according to $\Delta S^{\circ}_{mix} = N \cdot R \cdot \ln(1/55.5) + R(N \cdot \ln(N))$, where R is the universal gas constant, N the number of interacting epitopes, and 1/55.5 represents the molar fraction of 1 mol of substance in 1 L of water.[29] As a result, at 25 °C this corresponds to a $-T\Delta S^{\circ}_{mix}$ of $10.0\ kJ \cdot mol^{-1}$ for the monovalent ligand **19**, and 26.5 and $30.3\ kJ \cdot mol^{-1}$ for the tetravalent **24** and hexavalent **28**, respectively.

In summary, the solvation entropy $-T\Delta S_{solv}$ should increase with valency and remains rather constant per epitope and oligovalent ligands benefit from reduced mixing entropies $-T\Delta S^{\circ}_{mix}$ per epitope. On the other hand, the conformational entropy $-T\Delta S_{conf}$ is determined by linker geometry and difficult to predict but seems to be the main source for entropy penalties. The normalized entropy penalties ($T\Delta S^{\circ}$/epitope $= 18.9 \pm 4.9\ kJ \cdot mol^{-1}$) for di- to hexavalent ligands differ generally according to valency, scaffold flexibility (from linear, branched, cyclic to aromatic), and numbers of rotational bonds per epitope (from 2 to 6). Surprisingly, however, the scaffold does not have a strong influence on activity, whereas the valency of the ligands has a dominant impact. Hence, this opens the possibility to influence pharmacokinetic properties of the ligands, such as solubility, polarity or metabolic stability, via the scaffold structure.

Table 3: Compounds tested in the immune cell assay and their dissociation constants. Structures of the monomers **3** and **34**,[18b] tetravalent ligand **24**, hexavalent ligand **28** and glycopolymer **33**. Ligands **24** and **28** are oligovalent versions and **33** is a polymeric version of **3** (without linker) and **19** (with linker).

Comp.	Structure	K_D[a] [μM]
3[18b]	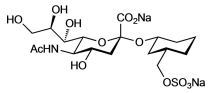	259
19	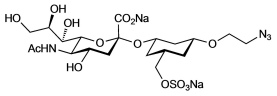	230
34[18b]	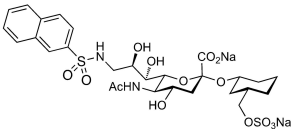	15
24	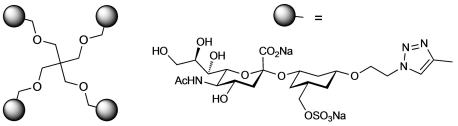	14.3
28	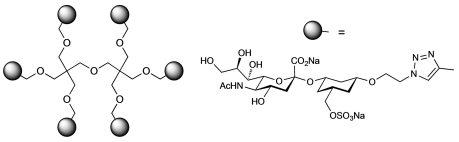	9.2
33	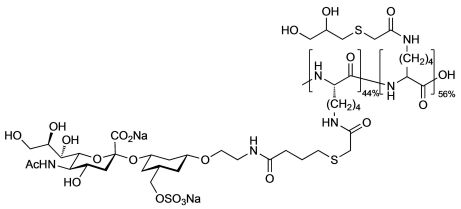	0.042
35[b]	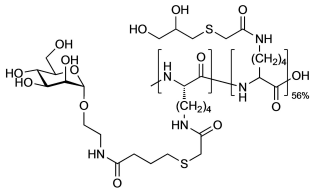	n.b.[c]

[a] Dissociation constants K_D were determined by ITC (see the Supporting Information for details). [b] Negative control. [c] n.b.: no binding.

Immune-Cell-Based Assay

The ability of a synthetic polyacrylamide conjugate displaying glycan ligands to bind to cells that express Siglec-8 was previously demonstrated by Bochner and co-workers.[11] To elucidate the effect of affinity and avidity of Siglec-8 ligands on the biological response, we compared the branched oligovalent compounds **24** and **28** and the poly-L-lysine glycopolymer **33** (PLL-**33**). In addition, the sulfonamide derivative **34**,[18b] which is 15 times more active than the epitope used for **24**, **28** and **33**, was chosen as monovalent test compound (Table 3). These four compounds were evaluated for their ability to modulate the activation of Siglec-8-expressing immune cells.

For testing the activity, we used Jurkat NFAT (Luc2) cells[30] that were transduced with Siglec-8. This reporter cell line possesses a firefly luciferase gene regulated by the transcription factor NFAT (Nuclear Factor of Activated T cells) that is activated by T cell receptor-mediated cell stimulation. Previous results have shown that the presence of inhibitory Siglecs such as Siglec-7 and Siglec-9 on these cells negatively influences the signaling cascade leading to the detection of a lower luciferase signal after activation.[30] In accordance with these finding, we found that Siglec-8-expressing Jurkat NFAT (Luc2) cells also showed a decreased luciferase signal when compared to control-transduced Jurkat cells (MOCK) upon stimulation with an

agonistic CD3 antibody (Figure 2A). Addition of the sulfonamide derivative **34** did not change the activation of MOCK or Siglec-8 Jurkat cells (Figure 2B). In contrast, the branched tetra-and hexavalent ligands **24** and **28** mediated an increased activation of Siglec-8 Jurkat cells, while there was no effect on MOCK control cells (Figure 2B). For the tetravalent ligand **24** this effect was dose dependent, with increasing concentrations resulting in stronger cell activation. Conversely, the hexavalent ligand **28** exerted the strongest effect at lower concentrations (Figure 2B). The glycopolymer **33** increased the activity of Siglec-8-expressing Jurkat cells, while there was no effect on the MOCK control cells (Figure 2C). To exclude any interference caused by the structure of the polymer itself, a PLL^{400}-based polymer displaying D-mannose (**35**, Man-PLL^{400}) instead of the sialic acid derivative **19** as binding epitope, and thereby unable to ligate Siglec-8, was used as negative control. Indeed, treatment with this polymer did not result in a signal change, confirming that the result with glycopolymer **33** was dependent on Siglec-8 ligation (Figure 2C). Due to the increased number of glycomimetic epitopes present in the glycopolymer **33** we used lower concentrations (pM range) compared to the μM concentrations of the branched oligovalent ligands **24** and **28**. When comparing the activities of the compounds after correcting for valency, that is, at the same ligand concentration (1 μM), the degree of activation correlates with valency (Figure 2D). Whereas glycopolymer **33** showed the strongest activation of Siglec-8-expressing Jurkat cells with a 3.3-fold increase in luminescence signal, the hexavalent compound **28** showed a slightly lower (2.6-fold) and the tetravalent compound **24** a 2-fold increase. Finally, sulfonamide derivative **34** had no effect. The slight increase in the activity of MOCK control cells in presence of the multivalent glycopolymer **33** could indicate that off-target effects may occur at higher concentrations (Figure 2D), which was not observed at lower concentrations (Figure 2C).

We further tested the role of *cis* ligands present on Jurkat cells on the activation potential of the tested Siglec-8 ligands. Therefore, we pre-treated Jurkat cells with sialidase to remove naturally expressed ligands before stimulating the cells in presence of glycopolymer **33**. In all cases, sialidase pre-treatment only led to a small increase in luciferase signal compared to the corresponding non-pre-treated situation (Figure 2E). Thus, sialidase pre-treatment only minimally influenced the inhibitory effect of glycopolymer **33** on Siglec-8-expressing Jurkat cells (Figure 2E).

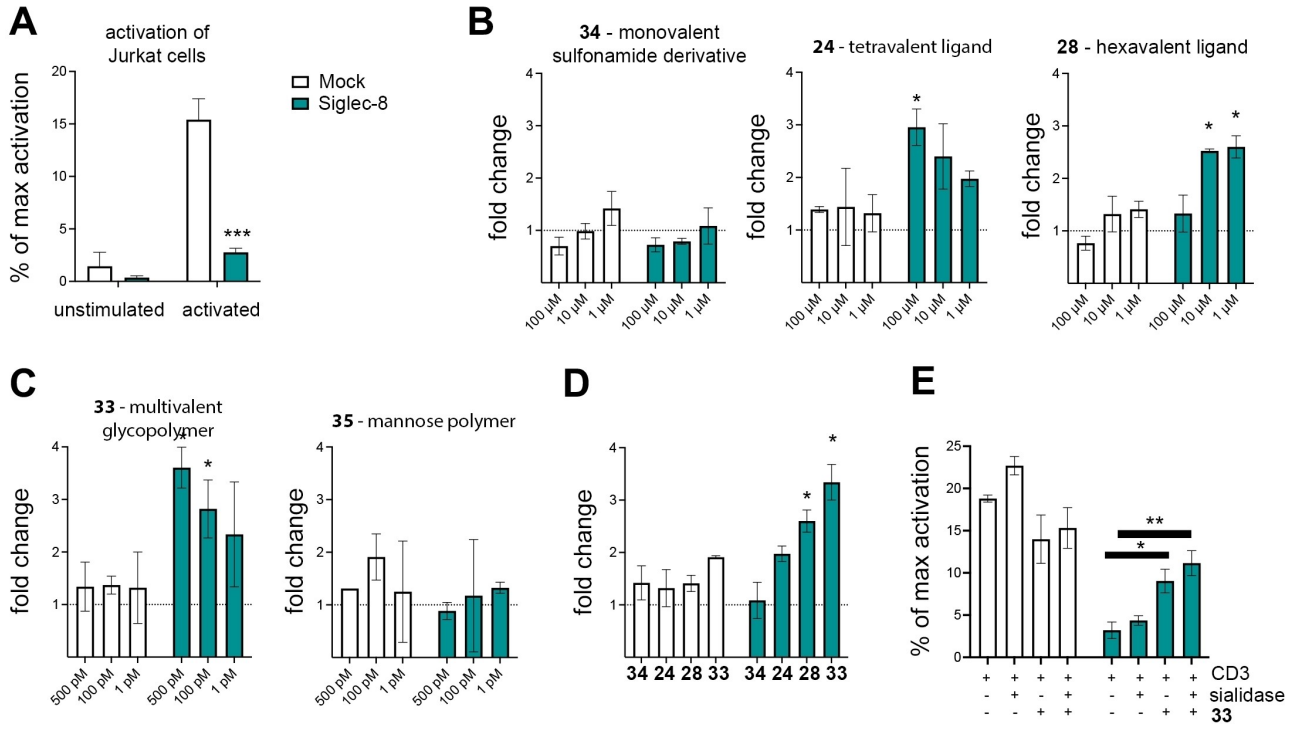

Figure 2. Multi- and oligovalent Siglec-8 glycomimetics reduce the inhibitory effect of Siglec-8 on immune cells. MOCK or Siglec-8 transduced Jurkat cells were left untreated (unstimulated) or activated with an activating CD3 antibody either in the absence or in the presence of Siglec-8 ligands at various concentrations. Activation of cells was measured by the luminescence signal induced after CD3 stimulation. A) Comparison of activation of Siglec-8-expressing Jurkat cells and MOCK controls. The luminescence signal was normalized to the maximum luminescence signal achieved by PMA/ionomycin stimulation. B–D) MOCK and Siglec-8 Jurkat cells were activated in the presence of monovalent mimetic **34**, tetravalent mimetic **24** and hexavalent mimetic **28** (B) or poly-L-lysine glycopolymer **33** in comparison to poly-L-lysine mannose polymer **35** as negative control (C). The activation with Siglec-8 ligands was normalized to the activation with CD3 alone (dashed line) for each cell line. D) Comparison of all Siglec-8 mimetics at a concentration of 1 μM. E) Siglec-8 and MOCK cells were treated with sialidase prior to activation with CD3 in presence or absence of glycomimetic **33** (500 pM). Statistical analysis was performed by a *t* test between Mock transfected and Siglec-8 transfected Jurkat cells. $*p < 0.05$, $**p < 0.01$. Bars represent means with SD of 2–3 independent experiments.

Overall, these results show that the oligovalent ligands **24** and **28** and the multivalent glycomimetic **33** bind Siglec-8 on Siglec-8-expressing Jurkat NFAT (Luc2) cells to cause an activation of Siglec-8 signaling. In contrast, the monovalent sulfonamide derivative **34** was not able to activate the immune cells, despite having a 17-fold higher affinity than the monovalent epitope **3** of the glycomimetics.

Conclusion

Siglecs are known to interact with glycans terminating in sialic acid on the same cell surface (through *cis* ligation) and to block interactions with lower affinity ligands, thereby setting a threshold for productive Siglec signaling.[31] To overcome this threshold, we produced and studied high-affinity oligo- and multivalent ligands that are able to compete with *cis* interactions.

The affinity of the preferred natural ligand 6′-sulfo-sLe^x (**1**) for Siglec-8 is only 279 μM.[16] In a first step, we structurally simplified the natural epitope to yield Siaα(2–3)-6-sulfo-GalOMe (**2**) with a K_D of 574 μM. Replacement of the 6-sulfo-GalOMe moiety by (1*R*,3*S*)-(3-hydroxycyclohexyl)methyl-1-sulfate yielded the Siglec-8 ligand **3** with a K_D of 259 μM.[18b]

The question remains, whether the mimetics **3** and **34** occupy the same binding pocket as their natural counterpart 6′-sulfo-sLe^x (**1**, PDB ID: 2N7B)[16] and the recently published 9-*N*-naphthylsulfonamide-Neu5Ac derivative (PDB ID: 7QUI).[32] Since both, glycomimetic **3** and **34** exhibit the same pharmacophore as the two compounds mentioned above, that is, the same molecular features necessary for molecular recognition, it can be assumed that they occupy the Siglec-8 binding site identically.

In this communication, a further affinity improvement was realized by oligo- and multivalent presentations of Siglec-8 ligand **3**. To enable its oligo- or multivalent presentation, a linker was introduced (→**19**, $K_D = 230$ μM). Subsequently, a special focus was laid on the type of scaffold employed (i.e., linear, cyclic, aromatic). When the oligovalent presentations of **19** (→**20**–**30**) were thermodynamically characterized, we found that the enthalpy contributions for each epitope were within a narrow range ($\Delta H°$/epitope = -27.8 ± 2.5 kJ·mol^{-1}). The normalized entropy penalties ($T\Delta S°$/epitope = 18.9 ± 4.9 kJ·mol^{-1}) for di- to hexavalent ligands differ generally according to valency, scaffold flexibility (from linear, branched, cyclic to aromatic), and numbers of rotational bonds per epitope (from 2 to 6). Because the scaffold does not have a strong influence on activity, this opens the possibility to influence pharmacokinetic properties of the ligands, such as solubility, polarity or metabolic stability, via the scaffold structure.

Finally, mono-, tetra-, hexa- and multivalent Siglec-8 ligands were tested in an immune-cell-based bioassay to study their ability to bind to Siglec-8 and modulate immune activation. The monomeric glycomimetic **34** ($K_D = 15$ μM), was not able to activate Siglec-8 signaling, whereas the tetravalent ligand **24** exhibiting the same affinity showed a clear effect. Furthermore, the hexavalent ligand **28** induced receptor clustering to an even larger extent, reaching almost the capability of the multivalent ligand **33** (Figure 2D). In summary, not only synthetic polymers[10] or antibodies[9,11,12] but also tetravalent **24** and, even more pronounced, the hexavalent **28** were able to cluster Siglec-8 into microdomains, a process necessary for exerting an agonistic biological response. Small monovalent molecules, however, are not able to induce the formation of these microdomains and, therefore, only antagonistically bind the protein in positions they are present on the cell surface.

In a next step, the influence of epitope affinity (epitope **3** vs. epitope **34**) on the biological response will be investigated. In addition, further studies with cells naturally expressing Siglec-8 will need to be conducted to test the effect of our novel oligovalent Siglec-8 ligands on Siglec-8-induced apoptosis of eosinophils and mast cells, because the Jurkat model used is highly artificial and only a limited number of natural ligands for *cis* interactions is present. Testing in primary cells will mark an important step towards the application of such molecules for the treatment of eosinophil- or mast-cell-associated disorders.

Supporting Information

The data that support the findings of this study are available in the supplementary material of this article.

Acknowledgements

This project has received funding from the European Union's Horizon 2020 research and innovation program under the Marie Skłodovska-Curie grant agreement No 765581. We also thank Dr. Pierre Thesmar (Organic Chemistry, Department of Chemistry, University of Basel), and Ad van der Eerden and Thomas Dezaire (Inorganic Chemistry and Catalysis, Department of Chemistry, Utrecht University) for their technical support in performing the hydrogenation at high pressure.

Conflict of Interest

The authors declare no conflict of interest.

Data Availability Statement

The data that support the findings of this study are available in the supplementary material of this article.

Keywords: Eosinophil-Associated Disorders · Glycomimetics · Low-Valency Ligands · Oligovalency · Siglec-8

[1] a) A. Varki, T. Angata, *Glycobiology* **2006**, *16*, 1R–27R; b) M. S. Macauley, P. R. Crocker, J. C. Paulson, *Nat. Rev. Immunol.* **2014**, *14*, 653–666.

[2] P. R. Crocker, J. C. Paulson, A. Varki, *Nat. Rev. Immunol.* **2007**, *7*, 255–266.
[3] J. V. Ravetch, L. L. Lanier, *Science* **2000**, *290*, 84–89.
[4] a) P. R. Crocker, P. Redelinghuys, *Biochem. Soc. Trans.* **2008**, *36*, 1467–1471; b) J. C. Paulson, M. S. Macauley, N. Kawasaki, *Ann. N.Y. Acad. Sci.* **2012**, *1253*, 37–48.
[5] B. E. Collins, O. Blixt, A. R. DeSieno, N. Bovin, J. D. Marth, J. C. Paulson, *Proc. Natl. Acad. Sci. USA.* **2004**, *101*, 6104–6109.
[6] B. E. Collins, O. Blixt, S. Han, B. Duong, H. Li, J. K. Nathan, N. Bovin, J. C. Paulson, *J. Immunol.* **2006**, *177*, 2994–3003.
[7] A. Gonzales-Gil, T. A. Li, R. L. Schnaar, *Mol. Aspects Med.* **2023**, *90*, 101110.
[8] a) B. A. Youngblood, J. Leung, R. Falahati, J. Williams, J. Schanin, E. C. Brock, B. Singh, A. T. Chang, J. A. O'Sullivan, R. P. Schleimer, N. Tomasevic, C. R. Bebbington, B. S. Bochner, *Cells* **2021**, *10*, 19–32; b) T. Kiwamoto, N. Kawasaki, J. C. Paulson, B. S. Bochner, *Pharmacol. Ther.* **2012**, *135*, 327–336.
[9] J. Schanin, S. Gebremeskel, W. Korver, R. Falahati, M. Butuci, T. J. Haw, P. M. Nair, G. Liu, N. G. Handsbro, P. M. Hansbro, E. Eversen, E. C. Brock, A. Xu, A. Wong, J. Leung, C. Bebbington, N. Tomasevic, B. A. Youngblood, *Mucosal Immun.* **2021**, *14*, 366–376.
[10] a) C. D. Rillahan, E. Schwartz, C. Rademacher, R. McBride, J. Rangarajan, V. V. Fokin, J. C. Paulson, *ACS Chem. Biol.* **2013**, *8*, 1417–1422; b) A. A. Chinarev, O. E. Galanina, N. V. Bovin, *Methods Mol. Biol.* **2010**, *600*, 67–78; c) E. M. Rapoport, G. V. Pazynina, M. A. Sablina, P. R. Crocker, N. V. Bovin, *Biochem. (Moscow)* **2006**, *71*, 496–504; d) S. Duan, B. M. Arlian, C. M. Nycholat, Y. Wei, H. Tateno, S. A. Smith, M. S. Macauley, Z. Zhu, B. S. Bochner, J. C. Paulson, *J. Immunol.* **2021**, *206*, 2290–2300.
[11] S. A. Hudson, N. V. Bovin, R. L. Schnaar, P. R. Crocker, B. S. Bochner, *J. Pharmacol. Exp. Ther.* **2009**, *330*, 608–612.
[12] a) E. S. Dellon, K. A. Peterson, J. A. Murray, G. W. Falk, N. Gonsalves, M. Chehade, R. M. Genta, J. Leung, P. Khoury, A. D. Klion, S. Hazan, M. Vaezi, A. C. Bledsoe, S. R. Durrani, C. Wang, C. Shaw, A. T. Chang, B. Singh, A. P. Kamboj, H. S. Rasmussen, M. E. Rothenberg, I. Hirano, *N. Engl. J. Med.* **2020**, *383*, 1624–1634; b) B. A. Youngblood, E. C. Brock, J. Leung, R. Falahati, B. J. Bryce, J. Bright, J. Williams, L. D. Shultz, D. L. Greiner, M. A. Brehm, C. Bebbington, N. Tomasevic, *Int. Arch. Allergy Immunol.* **2019**, *180*, 91–102.
[13] Y. Jia, H. Yu, S. M. Fernandes, Y. Wei, A. Gonzalez-Gil, B. S. Bochner, R. C. Kern, R. P. Schleimer, R. L. Schnaar, *J. Allergy Clin. Immunol.* **2015**, *135*, 799–810.
[14] T. Angata, C. M. Nycholat, M. S. Macauley, *Trends Pharmacol. Sci.* **2015**, *36*, 645–660.
[15] a) B. S. Bochner, R. A. Alvarez, P. Mehta, N. V. Bovin, O. Blixt, J. R. White, R. L. Schnaar, *J. Biol. Chem.* **2005**, *280*, 4307–4312; b) H. Tateno, P. R. Crocker, J. C. Paulson, *Glycobiology* **2005**, *15*,1125–1135.
[16] J. M. Pröpster, F. Yang, S. Rabbani, B. Ernst, F. H.-T. Allain, M. Schubert, *Proc. Natl. Acad. Sci. USA* **2016**, *113*, E4170–E4179.
[17] a) H. H. M. Abdu-Allah, K. Watanabe, G. C. Completo, M. Sadagopan, K. Hayashizaki, C. Takaku, T. Tamanaka, H. Takematsu, Y. Kozutsumi, J. C. Paulson, T. Tsubata, H. Ando, H. Ishida, M. Kiso, *Bioorg. Med. Chem.* **2011**, *19*, 1966–1971; b) S. Mesch, K. Lemme, M. Wittwer, H. Koliwer-Brandl, O. Schwardt, S. Kelm, B. Ernst, *ChemMedChem* **2012**, *7*, 134–143; c) O. Schwardt, S. Kelm, B. Ernst, *Top. Curr. Chem.* **2015**, *367*, 151–200; d) H. Prescher, M. Frank, S. Gütgemann, E. Kuhfeldt, A. Schweizer, L. Nitschke, C. Watzl, R. Brossmer, *J. Med. Chem.* **2017**, *60*, 941–956.
[18] a) C. M. Nycholat, S. Duan, E. Knuplez, C. Worth, M. Elich, A. Yao, J. O'Sullivan, R. McBride, Y. Wei, S. M. Fernandes, Z. Zhu, R. L. Schnaar, B. S. Bochner, J. C. Paulson, *J. Am. Chem. Soc.* **2019**, *141*, 14032–14037; b) B. S. Kroezen, G. Conti, B. Girardi, J. Cramer, X. Jiang, S. Rabbani, J. Müller, M. Kokot, E. Luisoni, D. Ricklin, O. Schwardt, B. Ernst, *ChemMedChem* **2020**, *15*, 1706–1719.
[19] a) R. J. Pieters, *Org. Biomol. Chem.* **2009**, *7*, 2013–2025; b) J. J. Lundquist, E. J. Toone, *Chem. Rev.* **2002**, *102*, 555–578; c) W. Lu, R. J. Pieters, *Expert Opin. Drug Discovery* **2019**, *14*, 387–395.
[20] a) B. Wagner, F. P. C. Binder, X. Jiang, T. Mühlethaler, R. C. Preston, S. Rabbani, M. Smieško, O. Schwardt, B. Ernst, *Molecules* **2023**, *28*, 2595–2604; b) D. Rotticci, T. Norin, K. Hult, *Org. Lett.* **2000**, *2*, 1373–1376; c) R. Ter Halle, Y. Bernet, S. Billard, C. Bufferne, P. Carlier, C. Delaitre, C. Flouzat, G. Humbolt, J. C. Laigle, F. Lombard, S. Wilmouth, *Org. Process Res. Dev.* **2004**, *8*, 283–286.
[21] Y. Zhao, Y. Wu, P. De Clercq, M. Vandewalle, P. Maillos, J. C. Pascal, *Tetrahedron: Asymmetry* **2000**, *11*, 3887–3900.
[22] S. P. Fritz, *Synlett* **2012**, *23*, 480–481.
[23] C. S. Chao, M. C. Chen, S. C. Lin, K. K. T. Mong, *Carbohydr. Res.* **2008**, *343*, 957–964.
[24] H. C. Kolb, M. G. Finn, K. B. Sharpless, *Angew. Chem. Int. Ed.* **2001**, *40*, 2004–2021.
[25] T. R. Chan, R. Hilgraf, K. B. Sharpless, V. V. Fokin, *Org. Lett.* **2004**, *6*, 2853–2855.
[26] a) J. Cramer, B. Aliu, X. Jiang, T. Sharpe, L. Pang, A. Hadorn, S. Rabbani, B. Ernst, *ChemMedChem* **2021**, *16*, 2345–2353; b) J. Cramer, A. Lakkaichi, B. Aliu, R. P. Jakob, S. Klein, J. Cattaneo, X. Jiang, S. Rabbani, O. Schwardt, G. Zimmer, M. Ciancaglini, T. Abreu Mota, T. Maier, B. Ernst, *J. Am. Chem. Soc.* **2021**, *143*, 17465–17478.
[27] F. H. Niesen, H. Berglund, M. Vedadi, *Nat. Protoc.* **2007**, *2*, 2212–2221.
[28] J. D. Chodera, D. L. Mobley, *Annu. Rev. Biophys.* **2013**, *42*, 121–141.
[29] K. P. Murphy, D. Xie, K. S. Thompson, L. M. Amzel, E. Freire, *Proteins Struct. Funct. Bioinf.* **1994**, *18*, 63–67.
[30] Y. Ikehara, S. K. Ikehara, J. C. Paulson, *J. Biol. Chem.* **2004**, *279*, 43117–43125.
[31] N. Razi, A. Varki, *Proc. Natl. Acad. Sci. USA* **1998**, *95*, 7469–7474.
[32] M. P. Lenza, U. Atxabal, C. Nycholat, I. Oyenarte, A. Franconetti, J. I. Quintana, S. Delgado, R. Núñez-Franco, C. T. G. Marroquín, H. Coelho, L. Unione, G. Jiménez-Oses, F. Marcelo, M Schubert, J. C. Paulson, J. Jiménez-Barbero, J. Ereño-Orbe, *JACS Au* **2023**, *3*, 204–215.

Manuscript received: September 26, 2023
Accepted manuscript online: November 9, 2023
Version of record online: November 23, 2023